JACS
JOURNAL OF THE AMERICAN CHEMICAL SOCIETY

ARTICLE

pubs.acs.org/JACS

Promiscuity in Alkaline Phosphatase Superfamily. Unraveling Evolution through Molecular Simulations

Violeta López-Canut,[†] Maite Roca,[†] Juan Bertrán,[§] Vicent Moliner,[*,‡] and Iñaki Tuñón[*,†]

[†]Departament de Química Física, Universitat de València, 46100 Burjassot, Spain

[‡]Departament de Química Física i Analítica, Universitat Jaume I, 12071 Castellón, Spain

[§]Departament de Química, Universitat Autònoma de Barcelona, 08193 Bellaterra, Spain

Supporting Information

ABSTRACT: We here present a theoretical study of the alkaline hydrolysis of a phosphodiester (methyl *p*-nitrophenyl phosphate or MpNPP) in the active site of *Escherichia coli* alkaline phosphatase (AP), a monoesterase that also presents promiscuous activity as a diesterase. The analysis of our simulations, carried out by means of molecular dynamics (MD) simulations with hybrid quantum mechanics/molecular mechanics (QM/MM) potentials, shows that the reaction takes place through a D_NA_N or dissociative mechanism, the same mechanism employed by AP in the hydrolysis of monoesters. The promiscuous activity observed in this superfamily can be then explained on the basis of a conserved reaction mechanism. According to our simulations the specialization in the hydrolysis of phosphomonoesters or phosphodiesters, developed in different members of the superfamily, is a consequence of the interactions established between the protein and the oxygen atoms of the phosphate group and, in particular, with the oxygen atom that bears the additional alkyl group when the substrate is a diester. A water molecule, belonging to the coordination shell of the Mg^{2+} ion, and residue Lys328 seem to play decisive roles stabilizing a phosphomonoester substrate, but the latter contributes to increase the energy barrier for the hydrolysis of phosphodiesters. Then, mutations affecting the nature or positioning of Lys328 lead to an increased diesterase activity in AP. Finally, the capacity of this enzymatic family to catalyze the reaction of phosphoesters having different leaving groups, or substrate promiscuity, is explained by the ability of the enzyme to stabilize different charge distributions in the leaving group using different interactions involving either one of the zinc centers or residues placed on the outer side of the catalytic site.

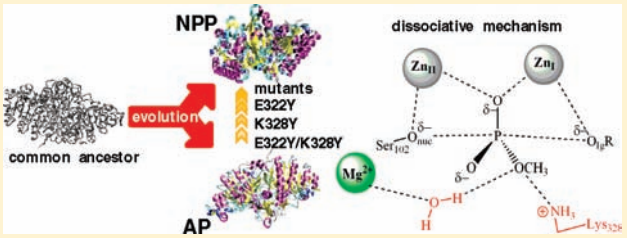

1. INTRODUCTION

Enzyme families can be grouped into evolutionarily related superfamilies. Frequently, members of a given superfamily have the ability to catalyze reactions of their evolutionary relatives.[1−4] These promiscuous activities provide new opportunities not only for designing new synthetic methodologies but also to test mechanistic hypotheses or the role of particular residues in a reaction and to understand the way followed by evolution to recruit and specialize enzymes for new functions. Structural similarities and promiscuous activities can be vestiges of evolutionary events with a common ancestor displaying broader catalytic activity.[5]

The alkaline phosphatase (AP) superfamily is a group of enzymes that catalyzes phosphoryl transfer reactions. This is a fundamental reaction in biochemical processes including energy storage, biosynthesis, or replication of genetic material.[6−10] Moreover, transphosphorylations are key regulatory mechanisms in cellular signaling.[11] Members of this group of enzymes include phosphomonoesterases, phosphodiesterases, phosphoglycerate mutases, phosphopentomutases, and sulfatases.[12−16] AP, the best characterized member of the superfamily, catalyzes phosphate monoesters hydrolysis, but it also shows secondary activity catalyzing phosphodiesters and related compounds.[5,16,17] A highly related member of this superfamily is the nucleotide pyrophosphatase/phosphodiesterase (NPP), an enzyme catalyzing phosphodiester hydrolysis,[18,19] but it also has secondary activity as phosphomonoesterase[20] and sulfatase.[21] Active sites of both AP and NPP have a clear structural relationship as can be seen in Figure 1. These sites contain two zinc ions and a deprotonated serine or threonine acting as a nucleophile. A prominent difference between AP and NPP is the presence of a third metallic ion in the former, a magnesium ion (Mg^{2+}) that could play a fundamental role in the discrimination between phosphate monoesters and diesters.[22] This ion was initially proposed to play a fundamental role in the deprotonation of the nucleophile.[23,24] However, the absence of this third ion in NPP and the lack of any other candidate to act as general base in this enzyme led to a reexamination of its role.[22] Recent studies with the E322Y mutant of *E. coli* AP in which one of the ligands of the magnesium ion was mutated, losing then the ability to bound this ion, showed that the absence of this metal center does not inactivate the enzyme completely.[22] This observation strongly suggests that the magnesium ion does not mediate general base catalysis. In addition, the

Received: February 25, 2011
Published: May 24, 2011

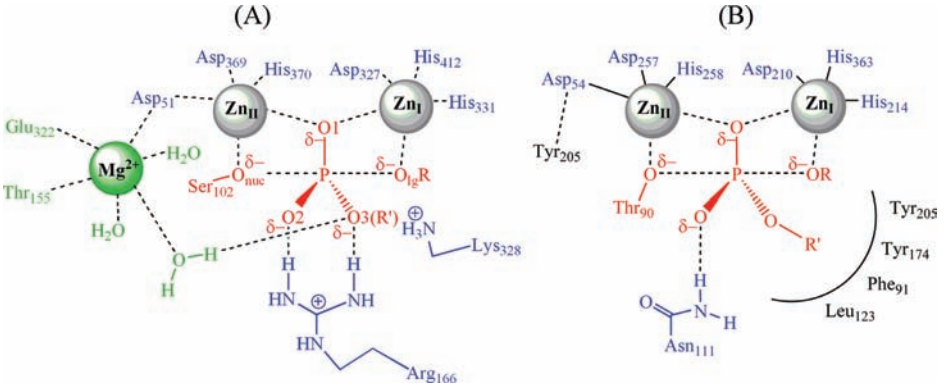

Figure 1. Schematic representation of the putative TS of the phosphomonoester and phosphodiester hydrolysis in the active sites of *Escherichia coli* AP (A) and *Xanthomonoas axonopodis pv. citri* NPP (B).

E322Y mutant showed a slightly increased activity with diesters, which offers an excellent opportunity to rationalize the specifi city differences between monoesterases and diesterases of the AP superfamily.[22]

Obviously, the role of the different constituents of the active sites must be established on the basis of the most accepted reaction mechanisms. In principle, phosphoester hydrolysis may proceed through dissociative or loose transition state (TS) structures, in which there is an advanced bond cleavage to the leaving group but no bond formation to the nucleophile, or through more associative or tight transition states (TSs), in which there is bond formation to the nucleophile and no bond cleavage to the leaving group.[8,25,26] Experimental studies[14,27] have established that AP catalyzes phosphomonoester hydrolysis through a dissociative or D_NA_N mechanism.[14,27] However, an analysis of kinetic isotope effects (KIEs) and linear free energy relationships (LFERs) found that the nature of the TS of AP catalyzed phosphodiester hydrolysis was more probably associative.[28] These studies then suggested that the AP enzyme is able to recognize and stabilize different TS's. The active site would be then flexible enough to be adapted to the characteristics of the chemical system, avoiding the energy penalty associated to a change in the nature of the TS.[5] However, the other way around has been also proposed to explain the promiscuous activity of related enzymes. In particular the promiscuous activity of protein phosphatase-1 with phosphonates has been explained on the basis of a mechanistic change when going from solution to the active site; this is assuming an evolutionary scenario in which the chemical system is adapted to the protein environment.[29]

In general, theoretical simulations of reaction processes are needed to determine the reaction mechanism in a more conclusive way. This is particularly interesting for the case of the phosphoester hydrolysis, where the interpretation of experimental data can be ambiguous due to the inherent difficulties associated to the flat nature of the free energy surface associated to these processes.[25] Methods based on hybrid quantum mechanics/molecular mechanics (QM/MM) potentials[30−33] are a powerful tool for studying chemical reactions in condensed phases such as solutions and enzyme active sites. In previous studies, we carried out QM/MM theoretical simulations of the AP activity with a benzyl phosphomonoester (*m*-nitrobenzyl phosphate or mNBP) finding that the chemical step is dissociative and stepwise. The breaking between the phosphorus and the leaving group was found to be the rate-limiting step,[34] in agreement with the interpretation of experimental data.[12] However, our recent theoretical simulations on a phosphodiester (methyl *p*-nitrophenyl phosphate or MpNPP) alkaline hydrolysis in aqueous solution and in the active site of NPP indicate that most probably a mechanistic change occurs when the system goes from one environment to another. Effectively, while the TS seems to be clearly associative in solution,[35] a dissociative mechanism is identified in the NPP active site.[36] Simulations show that electrostatic interactions in solution favor tight structures because the solvent reaction field reduces the repulsion between the negatively charged reacting species (nucleophile and substrate). Instead, the electrostatic features of the NPP active site stabilize the charge distribution of dissociative TS structures, in accordance with the structural similarity between AP and NPP active sites. Thus, our QM/MM studies would support a picture of evolution of the AP superfamily in which the reaction mechanism is maintained for different substrates.

If the reaction mechanism is the same for different members of the superfamily, then the question is now how the different specificities of AP and NPP for a particular substrate, phosphomonoesters or phosphodiesters, is attained. According to Herschlag and co-workers,[20,22] substrate specificity could be due to functional contacts to the substrate rather than from differences in the properties of the bimetallic site, which could induce changes in the reaction mechanism.[36] The main purpose of this paper is to investigate into the promiscuous ability of the AP enzyme to catalyze both the hydrolysis of phosphomonoesters and phosphodiesters and to rationalize the origin of the preference for the formers. We will analyze the hydrolysis reaction of a phosphodiester (methyl *p*-nitrophenyl phosphate diester, MpNPP) in the active site of AP, and the results will be compared with those obtained for the same substrate in NPP and for a phosphomonoester (*m*-nitrobenzylphosphate, mNBP) in AP. We will also show the results obtained for the same substrate in different AP mutants, including the E322Y AP mutant. We anticipate as a general conclusion that, in agreement with the predictions of Herschlag and co-workers, enzyme interactions with phosphate oxygen atoms play a decisive role to develop enzyme specificity within the AP superfamily.

2. METHODOLOGY

2.1. Wild Type Alkaline Phosphatase Models. The starting point for the study of the phosphodiesterase activity of AP was taken from our previous simulations on the hydrolysis of mNBP in this enzyme.[34] Details of the procedure followed are described elsewhere.[34]

Briefly, the X-ray crystal structure of *E. coli* AP with Protein Data Bank code 1ALK[23] was used as the starting geometry for the simulations. This structure is a homodimer with two active sites, both containing inorganic phosphate. The inorganic phosphate of one of the active sites was replaced by the substrate molecule (mNBP) while the other was kept empty. The protonation state of titatrable residues was calculated using the cluster method[37,38] assuming pH = 8, which is the optimum value for AP,[39] and verified using the PROPKA program.[40,41] We solvated the system with a water molecule sphere of 40 Å radius centered on the phosphorus atom of the substrate. Water molecules placed at less than 2.8 Å from any other non-hydrogen atom of the system were deleted. We defined as flexible all of those atoms belonging to residues or molecules found at a distance less or equal to 22 Å of the phosphorus atom. The system was then optimized and equilibrated by means of the combination of steepest-descent and conjugate gradient optimizations and molecular dynamics (MD) simulations.

In the present work a structure corresponding to the reactant state of mNBP hydrolysis was used as a template to model the reactant state of MpNPP hydrolysis. This phosphodiester was placed into the active site overlapping the phosphate groups with the uncharged oxygen atom bearing the methyl group (O3 in Figure 1A) oriented toward the Mg^{2+} site in agreement with the conclusions obtained by Herschlag and coworkers on the basis of their analysis of the reactivity of different enantiomers of a phosphorothioate diester.[22]

As found in our previous theoretical study in AP, a large QM subsystem is needed to reproduce the charge-transfer effects between the reactive system and the neighboring residues.[34] The QM region contains the Ser102 residue, the Arg166 residue, the Lys328 residue, the substrate (MpNPP), the two zinc ions, and their coordination spheres (Asp51, Asp369, His370, Asp327, His331, His412) (see Figure 1A). Because of the small size of the serine side chain, we included part of the previous and next residues of the protein sequence (Asp101 and Ala103) in the QM region. To saturate the valence of the QM/MM frontier we used the link atoms procedure,[42,43] placing these link atoms between the C_α and C_β atoms of each residue, except for residues Asp101 and Ala103 where the link atom was placed between the carbonyl carbon and C_α atoms. The number of QM atoms was 139. As in previous studies,[34−36,44,45] we used the semiempirical Hamiltonian AM1/d-PhoT (hereafter simply named as AM1d)[44] to describe the QM region. This Hamiltonian incorporates d-extension for the phosphorus atom and modified AM1 parameters for oxygen and hydrogen atoms, while the remaining atoms are described at the AM1 level. The MM region was described by means of the OPLS-AA[46,47] and TIP3P[48] potentials as implemented in the fDYNAMO library.[49]

This system was then optimized, combining steepest-descent and conjugate gradient steps. The total system consists of 30 190 atoms, of which 21 924 atoms were kept frozen during all of the subsequent simulations (those belonging to residues or molecules placed more than 22 Å away of the phosphorus atom). A switched cutoff, from 14 to 16 Å, was employed for all nonbonded MM interactions (including the frozen atoms), while the QM region was allowed to interact with every flexible MM atom. MD simulations were performed in the reactant state to warm up the system from 0 to 300 K. Finally, the system was equilibrated at 300 K using the NVT ensemble and the Langevin−Verlet integrator with a time step of 1 fs. The total simulation time employed to equilibrate the system was 300 ps. All of the QM/MM calculations were carried out using fDYNAMO.[49]

2.2. Alkaline Phosphatase Mutants. We also study the MpNPP hydrolysis in the active site of the E322Y AP mutant using the crystal structure with Protein Data Bank code 3DYC[22] as the starting geometry for the simulations. The protonation state of titratable residues at pH = 8 was determined using the PROPKA program.[40,41] The protein was solvated with a water molecule sphere of 40 Å radius centered on the phosphorus atom of the substrate, and the flexible region was defined containing all of the atoms of residues or molecules within a sphere of 22 Å radius centered on the phosphorus atom. The total system, which contains 30 259 atoms, of which 21 934 were kept frozen, was optimized by means of the combination of steepest-descent and conjugate gradient optimizations and warmed up to 300 K with a series of MD simulations. Finally, the system was equilibrated at 300 K using the NVT ensemble and the Langevin−Verlet integrator with a time step of 1 fs during a total simulation time of 300 ps.

Comparing the active sites of AP and NPP, other mutations of residues of the AP active site were proposed to improve its secondary activity as phosphodiesterase. The first mutant was designed replacing Lys328 of wild type AP (WT AP) by a tyrosine (K328Y AP), while a second one was designed replacing Lys328 by a tyrosine in the active site of the E322Y AP mutant (E322Y/K328Y AP). The same protocol described above was followed. The equilibration time in these mutants was longer (500 ps) to allow the system to relax after introducing the mutation in the X-ray structures of WT AP and E322Y AP mutant.

In all of the mutants, the QM region was defined as described above, using the AM1d Hamiltonian, whereas the rest of the system was treated by means of the OPLS-AA and TIP3P force fields. The total number of QM atoms was 139 when residue 328 is a lysine and 138 when this residue is replaced by tyrosine.

2.3. Potentials of Mean Force. To analyze the energetics of the chemical reaction, we performed the potential of mean force (PMF)[50] in all of the systems previously prepared at a reference temperature of 300 K. The antisymmetric combination of the distances describing the breaking and forming bonds [$d(P-O_{lg}) - d(P-O_{nuc})$, see Figure 1A for atom labeling] was employed as the distinguished reaction coordinate (RC). The umbrella sampling approach[51] was used to constraint the system close to a particular value of the reaction coordinate by means of the addition of a harmonic potential with a force constant of 2500 $kJ \cdot mol^{-1} \cdot Å^{-2}$. The probability distributions, obtained from a MD simulation within each individual window, are put together by means of the weighted histogram analysis method (WHAM)[52] to obtain the full probability distribution along the reaction coordinate. Each window consisted of 10 ps of equilibration followed by 15 ps of production. The total number of windows employed to cover the whole range of the reaction coordinate in all of the enzymatic systems were around 200, with small variations in each enzymatic system.

As in our previous study,[36] we also performed a two-dimensional PMF (2D-PMF) for the MpNPP hydrolysis in the AP active site to verify the associative/dissociative nature of the reaction mechanism obtained from the one-dimensional PMF. The 2D-PMF at a reference temperature of 300 K was performed as a function of the two distances corresponding to the breaking and forming bonds ($d(P-O_{lg})$ and $(P-O_{nuc})$) treated independently. We employed 630 windows to generate the 2D-PMF, and each window consisted of 10 ps of equilibration and 15 ps of production. The force constant applied to both distances was 2000 $kJ \cdot mol^{-1} \cdot Å^{-2}$.

2.4. Comparison between Theoretical and Experimental Free Energy Barriers. The comparison of experimental and theoretical kinetic data is particularly complicated in this superfamily. Inorganic phosphate, the product of the hydrolysis reaction, is a very efficient inhibitor of the enzymatic activity. This effect is the origin of the poor agreement between the kinetic constants (k_{cat} and K_M) determined in independent studies where saturating concentrations of inorganic phosphate were required to have appreciable changes upon hydrolysis.[39] Well-converged values of kinetic constants were determined only after the development of high sensitivity ^{32}P-based methods, able to work below the range where product inhibition occurs.[39] Unfortunately, under saturation conditions only k_{cat}/K_M can be measured. This provides the free energy barrier as measured from the ground state of the free enzyme and substrate in solution ($\Delta G_E^{\ddagger}$), while theoretical simulations are carried out from the substrate-enzyme Michaelis complex, providing a different

Scheme 1

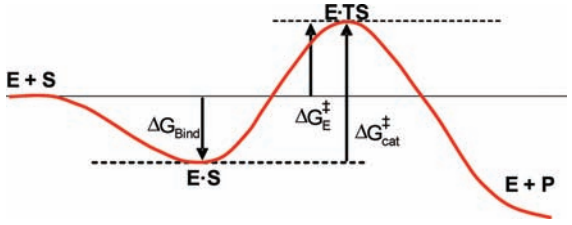

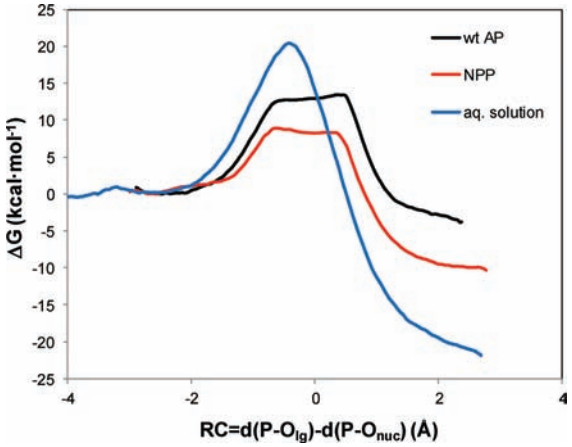

Figure 2. PMF obtained for the alkaline hydrolysis of MpNPP in aqueous solution, NPP, and WT AP.

value of the free energy barrier ($\Delta G^{\ddagger}_{cat}$). As shown in Scheme 1 and eq 1, both quantities are related through the binding free energy of the substrate

$$\Delta G_{cat}{}^{\ddagger} = \Delta G_{E}{}^{\ddagger} - \Delta G_{Bind} \quad (1)$$

3. RESULTS AND DISCUSSION

3.1. Reaction Mechanisms of Phosphodiester Hydrolysis in AP. In previous studies we used the QM/MM methodology described before to investigate the reaction mechanisms of the alkaline hydrolysis of MpNPP in aqueous solution and in the active site of NPP.[35,36] Our results showed a mechanistic change when going from aqueous solution to the NPP active site: a tight TS was obtained in solution while a much looser or dissociative TS was found in the enzyme. These differences where rationalized in terms of the very different nature of the electrostatic interactions established between the chemical system and the surroundings in these two environments. In aqueous solution the electric field acting on the system is a reaction field that essentially reduces the repulsion between the two negatively charged reaction fragments (the hydroxide anion and MpNPP) by a factor roughly equal to the dielectric constant. Then, if the electrostatic repulsion is diminished, chemical forces dominate the process, and an associative pathway is obtained. In the NPP active site the situation is quite different. There are no free rotating dipoles able to be adapted to any change in the charge distribution of the reacting fragment and to produce a reaction field. Instead, we have a much more permanent electric field

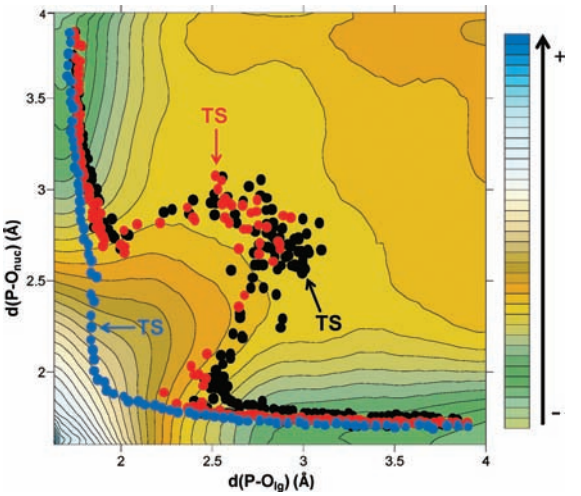

Figure 3. Averaged values of the P−O_{nuc} and P−O_{lg} distances found during the reaction PMFs for the alkaline hydrolysis of MpNPP in solution (blue), in the NPP active site (red), and in the WT AP active site (black) projected on the 2D-PMF obtained for the latter. The arrows point to the TS locations.

designed by evolution to stabilize the charge distribution of a dissociative TS.

In this work, we have carried out the simulations corresponding to the hydrolysis of MpNPP in the AP active site. We obtained a one-dimensional PMF using the antisymmetric combination of the distances from the phosphorus atom to the nucleophile and from the phosphorus atom to the leaving group [RC = d(P−O_{lg}) − d(P−O_{nuc})]. The resulting free energy profile, together with those previously obtained in aqueous solution and in NPP active site, is presented in Figure 2. The shape of the free energy profile is quite similar to that obtained in NPP: it presents a plateau around the TS region, while the profile in solution displays a bell-shaped curve. This difference is attributed to a change in the mechanism, from associative in aqueous solution to dissociative in both enzymatic active sites. Reaction mechanisms can be analyzed by means of the averaged P−O_{lg} and P−O_{nuc} distances obtained along the free energy profiles, as shown in Figure 3. These averaged distances have been drawn on the 2D-PMF obtained for the AP enzymatic reaction, as described in the previous section. This figure confirms the fact that the reaction mechanism in solution is associative, while it is dissociative in the two enzymatic active sites. Initially, the reaction is described, in all environments, as an approach of the nucleophile to the phosphorus atom while the leaving group remains strongly bonded. In aqueous solution the reaction continues without appreciable changes in the P−O_{lg} distance until the formation of a transient compact pentacoordinated structure with distances to the leaving and nucleophilic oxygen atoms of about 1.9 Å. The bond between the phosphorus atom and the leaving group oxygen atom is broken only after this tight structure is formed. In both AP and NPP enzymes, the reaction proceeds in a completely different way; the cleavage of the P−O_{lg} bond begins in a much earlier stage of the reaction, in such a way that the system reaches regions where both distances (P−O_{nuc} and P−O_{lg}) correspond to nearly broken bonds (around 2.8 Å), forming a transient tricoordinated structure. Once the new P−O_{nuc} bond has been formed, the distance between the phosphorus atom and the leaving group increases again. The 2D-PMF confirms this

dx.doi.org/10.1021/ja2017575 |J. Am. Chem. Soc. 2011, 133, 12050–12062

Table 1. Free Energy Barriers Computed at AM1d/MM Level for the MpNPP Hydrolysis (in kcal·mol^{-1}) and Relevant Averaged Distances (in Å)

	aqueous solution[a]		NPP[b]		AP	
	reactants	TS	reactants	TS	reactants	TS
$\Delta G^{\ddagger}_{AM1d/MM}$	0.0	20.5	0.0	8.9	0.0	13.5
$(P-O_{lg})$	1.67 ± 0.03	1.81 ± 0.05	1.71 ± 0.03	2.53 ± 0.10	1.69 ± 0.04	2.68 ± 0.11
$d(P-O_{nuc})$	∞	2.23 ± 0.06	4.59 ± 0.05	3.13 ± 0.10	4.16 ± 0.05	2.32 ± 0.11
$d(O_{nuc}\text{-}O_{lg})$	∞	4.03 ± 0.10	6.03 ± 0.11	5.57 ± 0.19	5.52 ± 0.09	4.92 ± 0.22
$d(P-O_{lg}) - d(P-O_{nuc})$	$-\infty$	-0.43	-2.88	-0.60	-2.47	0.36
$d(P-O_{lg}) + d(P-O_{nuc})$	∞	4.05	6.29	5.66	5.85	5.00

[a] From ref 35. [b] From ref 36.

dissociative or D_NA_N mechanism as the only available for the hydrolysis of MpNPP in the AP active site. An associative A_ND_N pathway, as the one observed in solution, would cross through regions with higher free energies. According to these results, and assuming an equilibrium distribution, reactive trajectories crossing through the associative region of the 2D-surface would be much less probable than trajectories across the region defining the dissociative mechanism.

Averaged distances from the phosphorus atom to the nucleophile and the leaving group for the TS's and the reactants are provided in Table 1 for the three profiles. The geometries of the TS's, in particular the value of the sum of the bond distances from the phosphorus atom to the nucleophile and leaving group oxygen atoms, confirm the different nature of the reaction mechanism in solution and in the enzymes. This is further confirmed from the analysis of the Pauling bond orders[53] of the phosphorus atom to the oxygen atoms of the leaving group and the nucleophile at the TS. In aqueous solution these bond orders are 0.83 and 0.46, respectively; for the reaction in NPP we obtained 0.32 and 0.14, and for the reaction catalyzed by AP we obtained 0.17 and 0.29. That is, the sum of the TS bond orders is larger than one in aqueous solution (1.29) and lower than one for the reaction in NPP and AP (0.46 in both cases), confirming the associative nature of the mechanism in solution and the dissociative mechanism in the enzymes.

The free energy barrier ordering obtained from the monodimensional PMF agrees with the expected behavior: 20.5 kcal·mol^{-1} for the aqueous solution reaction, 13.5 kcal·mol^{-1} for the reaction in AP, and 8.9 kcal·mol^{-1} for the reaction in NPP. That is, the value obtained for the hydrolysis of the phosphodiester in AP is in between the free energy barriers of the uncatalyzed process and the reaction catalyzed by its natural enzyme: AP catalyzes the hydrolysis of phosphodiesters but less efficiently than NPP. It must be noted that the AM1d/MM methodology employed here has been shown to produce slightly underestimated free energy barriers.[35,36] The predicted activation free energy in aqueous solution is in reasonable agreement with the activation free energy derived from application of TS theory to the experimental rate constant measured in solution at 42 °C, 25.9 kcal·mol^{-1}.[5] With respect to the enzymatic process, the calculated free energy barrier for the reaction in NPP is 4.6 kcal·mol^{-1} lower than in AP (see Table 1), which seems a reasonable estimation according to the experimental observation of a faster reaction in the former than in the latter. Moreover, the free energy barrier estimated using the same QM/MM methodology for the departure of the leaving group in the stepwise mechanism of mNBP hydrolysis in AP was 10.2 kcal·mol^{-1},[34] which is 3.3 kcal·mol^{-1} lower than for MpNPP, in agreement with the fact that AP is a better monoesterase than diesterase. The experimental second-order rate constants (k_{cat}/K_M) for the enzymatic reaction of mNBP and MpNPP in the presence of AP (1.8×10^7 and 18 M^{-1}·s^{-1}, respectively)[22] can be translated to a free energy barrier difference (estimated from free enzyme and substrate) using the following relationship:

$$\Delta\Delta G^{\ddagger}_{E} = \Delta G^{\ddagger}_{E,\,MpNPP} - \Delta G^{\ddagger}_{E,\,mNBP} = -RT \ln \frac{\left(\frac{k_{cat}}{K_M}\right)_{MpNPP}}{\left(\frac{k_{cat}}{K_M}\right)_{mNBP}} \quad (2)$$

According to eq 2 and using the experimentally determined rate constants, the free energy barrier $\Delta G^{\ddagger}_{E}$ is reduced by 8.2 kcal·mol^{-1} when going from the diester to the monoester. If we assume a more negative binding free energy for mNBP, which is the specific substrate of AP (this is, $\Delta\Delta G_{Bind} = \Delta G_{Bind,MpNPP} - \Delta G_{Bind,mNBP} > 0$), then the value provided by eq 2 should be an upper limit for the free energy barrier difference estimated from the Michaelis complex ($\Delta\Delta G^{\ddagger}_{cat}$, see eq 1), in agreement with the result of our simulations.

Figure 4 shows representative snapshots of the reactant state corresponding to the MpNPP and mNBP hydrolysis in AP and averaged values of some significant distances.[54] The MpNPP molecule was placed into the active site with the uncharged oxygen atom of the phosphate group (the one bearing the methyl group, O3) oriented toward the Mg^{2+} site, following the conclusions of Herschlag and co-workers.[22] We tried different conformations for the methyl group, rotating around the P−O-(R′) bond. In all cases we found that the methyl group was finally placed as shown in Figure 4. This methyl group is placed in such a way that establishes a C−H···O$^-$ hydrogen bond with the nucleophilic oxygen atom of Ser102. This kind of hydrogen-bond interaction has been documented for other systems, and it has been well-characterized with theoretical methods.[55,56] We checked the performance of the AM1d Hamiltonian to treat these interactions comparing the results obtained for a model system ($H_3CH\cdots OH^-$) with higher level calculations: M06−2X[57] and MP2[58,59] with the 6-311++G(2df,2p) basis set. The H···O distance and the interaction energies obtained with the semiempirical Hamiltonian (1.87 Å and −6.28 kcal·mol^{-1}) were in quite good agreement with those obtained at the M06−2X level (1.97 Å and −7.15 kcal·mol^{-1}) and at the MP2 one (1.97 Å and −6.65 kcal·mol^{-1}).

As observed in Figure 4, one oxygen atom of the phosphate group (O1) establishes a strong interaction with the Zn(I) ion,

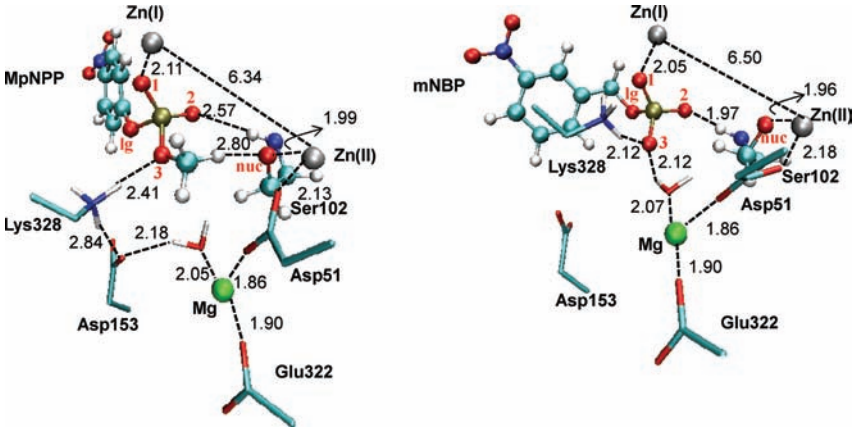

Figure 4. Representative snapshots of the reactant state of MpNPP (left) and mNBP (right) hydrolysis in the active site of AP. Averaged distances are given in Å.

Table 2. Averaged Mulliken Charges (in a.u.) Obtained for the Oxygen Atoms Bonded to the Phosphorous Atom in the Reactant and TS of the Hydrolysis of mNBP and MpNPP in AP[a]

	mNBP		MpNPP	
atom	reactants	TS	reactants	TS
O1	−1.07	−0.94	−0.51	−0.94
O2	−1.15	−1.08	−1.01	−0.99
O3	−1.10	−1.04	−0.55	−0.74
O_{lg}	−0.82	−0.83	−0.71	−0.65
O_{nuc}	−0.71	−0.74	−0.74	−0.81

[a] See Figure 1A for atom labeling.

while the O2 oxygen atom makes a hydrogen bond with the backbone amide of Ser102. Lys328 shows also a stabilizing contact with the oxygen atom bearing the methyl group (O3). Obviously, these interactions are much stronger in the case of a monoester since the negative charges on the oxygen atoms are larger. As shown in Table 2 the averaged Mulliken charges on the oxygen atom interacting with Zn(I) (O1) are −1.07 and −0.51 a.u. for the reactant states of mNBP and MpNPP, respectively. The corresponding charges on the oxygen atom interacting with the Ser102 amide group (O2) are −1.15 and −1.01 au, respectively. Finally the charges on O3 are −1.10 and −0.55 au for mNBP and MpNPP, respectively. This oxygen atom interacts in both cases with Lys328, but the averaged hydrogen bond distance is shorter for mNBP than for MpNPP (2.12 and 2.41 Å, respectively, see Figure 4). In the case of the monoester this oxygen atom also presents a hydrogen bond interaction with one water molecule belonging to the coordination shell of the Mg^{2+} center. This is one of the three structural water molecules, present in the X-ray structure,[23] that complete the coordination shell of the ion. These water molecules remain coordinated to the ion during all of the simulations. This interaction is not observed in the reactant state of MpNPP, where the water molecule interacts with Asp153, which in turn is hydrogen-bonded to Lys328. In the reactant state of mNBP, Asp153 is hydrogen-bonded to Arg166, not shown in Figure 4. Thus, and in agreement with the hypothesis of Herschlag and co-workers,[22] functional contacts to the substrate different to the bimetallic site contribute to the specificity difference between AP and

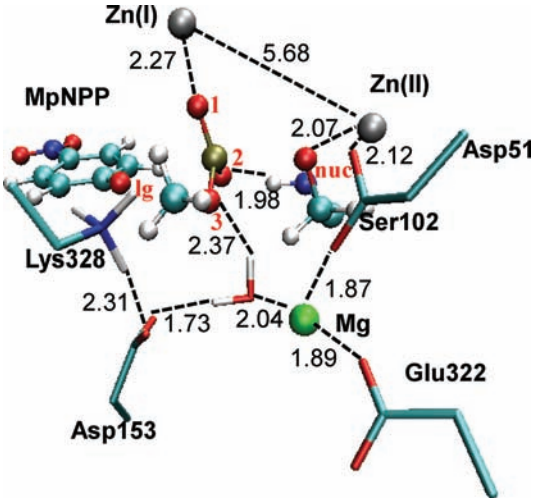

Figure 5. Representative snapshot of the TS for the MpNPP hydrolysis in the active site of AP. Averaged distances are given in angstroms (Å).

NPP. According to our structures, it seems that interactions with phosphate oxygen atoms, and in particular the differences observed when one of these oxygen atoms bears or not an alkyl group, could be determinants in understanding the preference of AP for phosphomonoesters. Finally, hydrogen bonds are also established between two oxygen atoms of the phosphate group in MpNPP and Arg166 (see Figure 1A and Figure S1 in the Supporting Information), but these hydrogen bonds are also observed in the case of the phosphomonoester.[34] Figure 4 also shows the distances of some residues involved in the coordination of the Mg^{2+} that will be important when analyzing the behavior of the E322Y mutant (see below).

Interactions contributing to the relative stabilization of the TS of MpNPP hydrolysis in AP can be identified comparing the averaged structure of the TS (see Figure 5) with that of the reactant state (Figure 4). The hydrogen bonds established between O2 and the amide group of Ser102 and between O3 and a water molecule of the coordination shell of the Mg^{2+} ion are reinforced when going from the reactant state to the TS. The first hydrogen bond is stronger than the second at the TS, not only because the distance is shorter (1.98 Å and 2.37 Å, respectively) but also because the averaged charge on the O2 atom is larger, in absolute

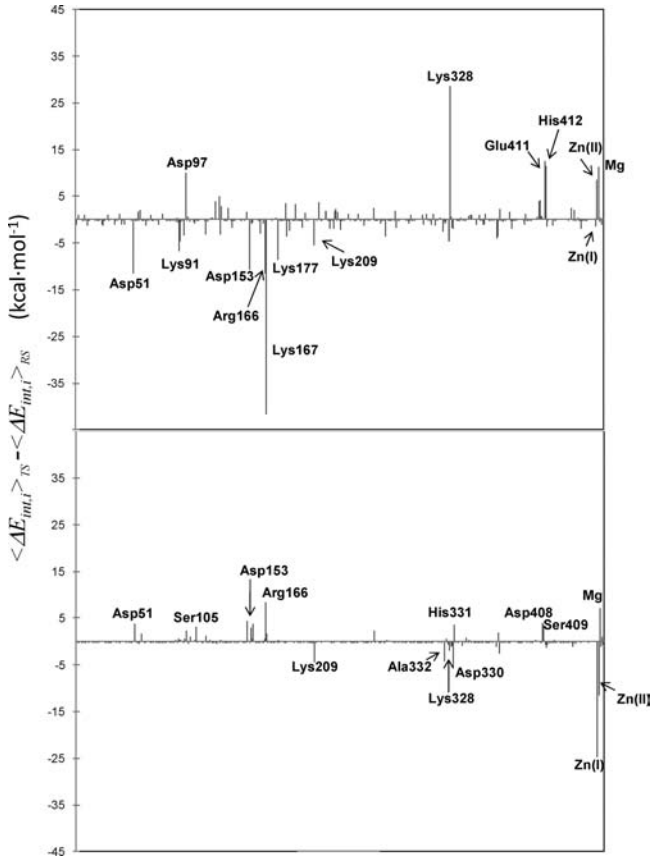

Figure 6. Averaged contribution of the interaction energy of each residue with the reacting system (ser102 + substrate) to the energy barrier of the MpNPP (A) and mNBP (B) hydrolysis in the active site of AP. Residues are ordered according to the sequence, and the metallic centers were added at the end.

value, than the charge of the O3 oxygen atom (−0.99 a.u. and −0.74 a.u., respectively, as seen in Table 2).

An important difference of the TS structure with respect to the reactant structure is the position of the methyl group. In the course of the reaction the phosphate group must be inverted and then the methyl group must break the interaction established with the nucleophilic oxygen atom. In addition, during the inversion process the methyl group is confronted to Lys328, which loses the interaction with the O3 oxygen atom. As discussed below, this interaction between the chemical system and Lys328 stabilizes the reactant state relatively to the TS, increasing the energy barrier of the diester hydrolysis. The position of Lys328 is held by means of a strong hydrogen bond established with Asp153, which, as explained before, is also hydrogen-bonded to a water molecule of the coordination shell of the Mg^{2+} ion and to Arg166.

To get a deeper insight into the impact of these and other residues in the catalytic activity of the enzyme, we computed the averaged contribution to the energy barrier of the interaction energy of each residue with the reacting system (Ser102 plus the MpNPP). This contribution is calculated as the difference of the interaction established in the transition and reactant state:

$$\langle \Delta E^{\ddagger}_{\mathrm{int,i}} \rangle = \langle E_{\mathrm{int,i}} \rangle_{\mathrm{TS}} - \langle E_{\mathrm{int,i}} \rangle_{\mathrm{RS}} \qquad (3)$$

where $\langle\rangle_{\mathrm{TS}}$ and $\langle\rangle_{\mathrm{RS}}$ denote averages over the transition and reactant states of the reaction, respectively, and the subscript i refers to the residues. The interaction energy of a particular residue with the reacting system was computed over 100 evenly spaced structures saved from a 100 ps QM/MM MD simulation in the reactant and transition states. The interaction energy includes both electrostatic and van der Waals terms. The electrostatic interactions are calculated treating the residues as a collection of point charges obtained either from the force field (if they belong to the MM subsystem) or from a Mulliken analysis (if they were originally included in the QM subsystem), while the reacting fragments are described at the AM1d level. The contribution of the interaction energy of each residue to the energy barrier is depicted in Figure 6. A negative value means that the interaction energy with this residue contributes to reduce the energy barrier, and a positive value means that contributes to increase it. It should be taken into account that the interaction energy with the reacting fragment does not provide the complete contribution of a given residue to the energy barrier, as far as it can also make a contribution through the interactions with other enzymatic fragments in the reactant and TS. Anyway, the quantities presented in Figure 6A may be useful to understand the catalytic properties of AP with MpNPP. The residues providing a more negative contribution of the interaction energy to the barrier are Arg166 and Lys167. The first is able to interact with two of the oxygen atoms of the phosphate group (O2 and O3), and this interaction is strengthened at the TS (see the evolution of the charges in Table 2). Lys167 is placed at the outer side of the active site and establishes a strong electrostatic interaction with the nitro group at the TS that presents an averaged Mulliken charge of −0.84 a.u. A figure showing the positioning of Arg166 and Lys167 at the reactants and TS together with the coordinates of the substrate and the most relevant residues for these two structures in PDB format are provided as Supporting Information (Figure S1). Other residues appearing with large negative contributions in Figure 6 are Asp51, Lys91, Asp153, Lys177, and Lys209. Their contributions can be rationalized in terms of the charge transfer taking place from the nucleophile to the leaving group and the large charge separation attained at the TS. The residue with the largest positive contribution, and then increasing the energy barrier, is Lys328. As mentioned before, this residue presents a hydrogen-bond interaction with the oxygen atom O3 at the reactant state, while it is confronted to the methyl group at the TS. Other residues making important positive contributions through the interaction energy are Asp97, Glu411, His412, and the metallic centers Zn(II) and Mg^{2+}. The Zn(II) and Mg^{2+} centers electrostatically stabilize the nucleophile in the reactant state. At the TS the charge separation in the reacting subsystem is larger, and then the net electrostatic effect of these two metallic centers is positive. It must be taken into account that the leaving group is able to delocalize the charge through the π-electronic system and the nitro group, and then the leaving group oxygen atom (O_{lg}) does not support a very large negative charge. This effect would also explain the small interaction energy contribution to decrease the barrier of the Zn(I) center. There are several points to be stressed when analyzing these data. First, as said before, the interaction energy is not the whole contribution of each residue (or metallic center) to the energy barrier. Second, in this analysis we are not considering the binding energy step, since we compare the TS to the Michaelis complex. Finally, it seems that AP is able to stabilize TS's using different strategies depending on the nature of the leaving group. So, when the substrate is MpNPP, the leaving group is able to delocalize the charge, and then Lys167 can play an important role in TS

Scheme 2

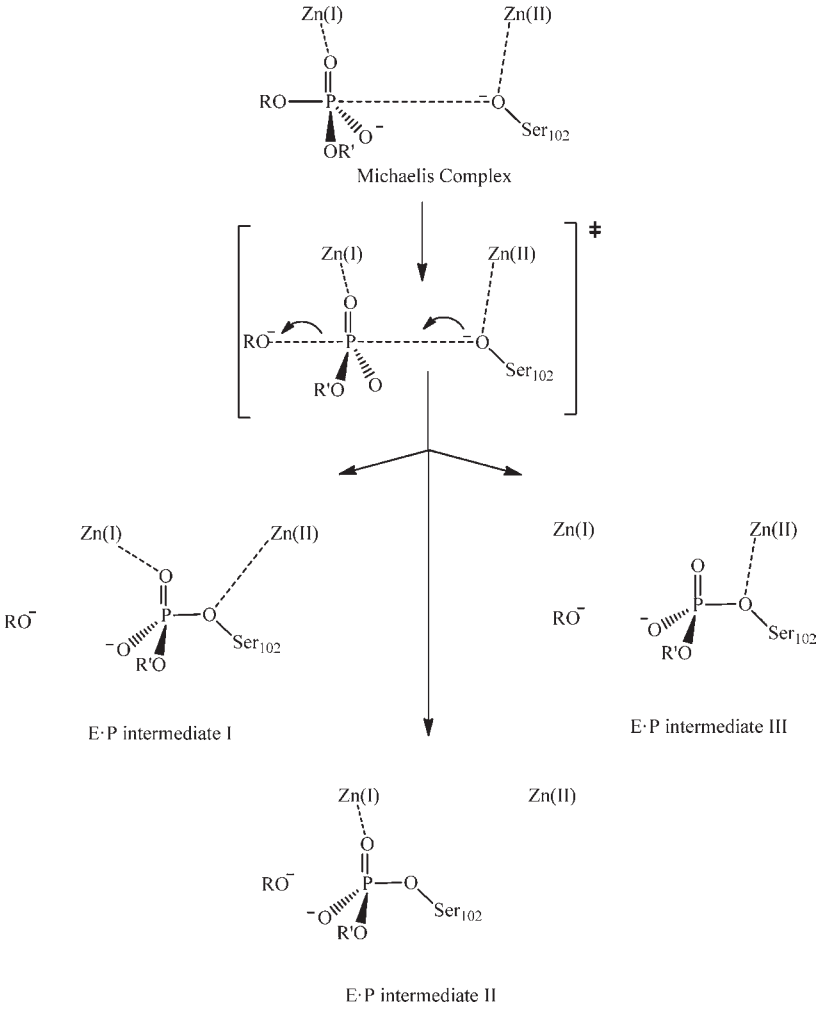

stabilization and not the Zn(I) ion. Instead, when the substrate has a worse leaving group, such as in the case of the hydrolysis of the mNBP monoester[34] or of the methyl phenyl phosphate diester,[36] Zn(I) can play a major role stabilizing the TS's, since the charge cannot be efficiently delocalized on the leaving group, and then a large fraction of this charge is now localized on the O_{lg} atom at the TS, as seen in Table 2. This is confirmed in the analysis of the interaction energies carried out for the hydrolysis of mNBP in AP, shown in Figure 6B. In this case the contributions of the interaction energy of both Zn centers with the reacting systems are negative (-24.8 and -11.5 kcal·mol^{-1} for Zn(I) and Zn(II), respectively), while the contribution of Lys167 is 1.6 kcal·mol^{-1}. Interestingly, these different strategies employed by AP to interact with the charge distribution of different TS's (through specific interactions with the phosphate group oxygen atoms or the leaving group), explain the substrate promiscuity displayed by the AP. In fact, this enzyme is able to catalyze the hydrolysis of phosphoesters with different leaving groups.[5,12,22] Another interesting difference between the contributions of the residues in the case of MpNPP and mNBP is found in Arg166. This residue plays a fundamental role in the binding process of the monoester, according to the interaction energy at the reactant state being -99.8 kcal·mol^{-1}, larger, in absolute value, than for the diester (-72.1 kcal·mol^{-1}). However, because of the charge delocalization found at the TS (see Table 2), the contribution to the barrier in the case of mNBP is positive (8.4 kcal·mol^{-1}).

After reaching the TS, the hydrolysis reaction of MpNPP in AP continues when Ser102 and the methylphosphate group mutually approach to form the new P$-O_{nuc}$ bond. During this approach both the nucleophile and the methylphosphate group remain bound to the zinc centers (Zn(II) and Zn(I) respectively). In this way, the covalent enzyme$-$methylphosphate intermediate obtained as a product of this reaction step is found in between the two zinc sites, as shown in Scheme 2 (E·P intermediate I).

3.2. Phosphodiester Hydrolysis in AP Mutants. Glu322 is one of the residues belonging to the coordination shell of the Mg^{2+} ion in AP. In NPP, Tyr205 occupies the region corresponding to the Mg^{2+} site (see Figure 1). Herschlag and co-workers prepared a mutant of AP with Glu322 replaced by tyrosine (E322Y AP). Since this mutant does not contain a Mg^{2+} ion, the active site is closer to that of NPP. According to the structural changes, the E322Y mutation produced a differential effect on monoesters and diesters hydrolysis. The value of k_{cat}/K_M for the reaction of E322Y AP with MpNPP is slightly increased with respect to the value determined for WT AP (35 and 18 $M^{-1}\cdot s^{-1}$ at 25 °C, respectively) which can be converted into a free energy barrier lowering ($\Delta\Delta G_E^{\ddagger}$) of approximately 0.4 kcal·mol^{-1}. Instead, the value of k_{cat}/K_M for the hydrolysis of mNBP is

dx.doi.org/10.1021/ja2017575 |J. Am. Chem. Soc. 2011, 133, 12050–12062

Table 3. Free Energy Barriers Computed at the AM1d/MM Level (in kcal·mol^{-1}) and Averaged Distances (in Å) for the MpNPP Hydrolysis in Different AP Mutants

	E322Y		K328Y		E322Y/K328Y	
	reactants	TS	reactants	TS	reactants	TS
$\Delta G^{\ddagger}_{AM1d/MM}$	0.0	12.1	0.0	12.0	0.0	9.1
(P−O_{lg})	1.71 ± 0.04	2.48 ± 0.15	1.69 ± 0.03	2.37 ± 0.14	1.72 ± 0.04	2.08 ± 0.15
d(P−O_{nuc})	4.25 ± 0.06	3.08 ± 0.15	4.36 ± 0.05	3.00 ± 0.14	4.86 ± 0.06	3.01 ± 0.14
d(O_{nuc}-O_{lg})	5.89 ± 0.08	5.42 ± 0.27	5.65 ± 0.16	5.21 ± 0.26	6.14 ± 0.12	4.98 ± 0.26
d(P−O_{lg}) − d(P−O_{nuc})	−2.54	−0.60	−2.67	−0.63	−3.14	−0.91
d(P−O_{lg}) + d(P−O_{nuc})	5.96	5.56	6.05	5.37	6.58	5.09

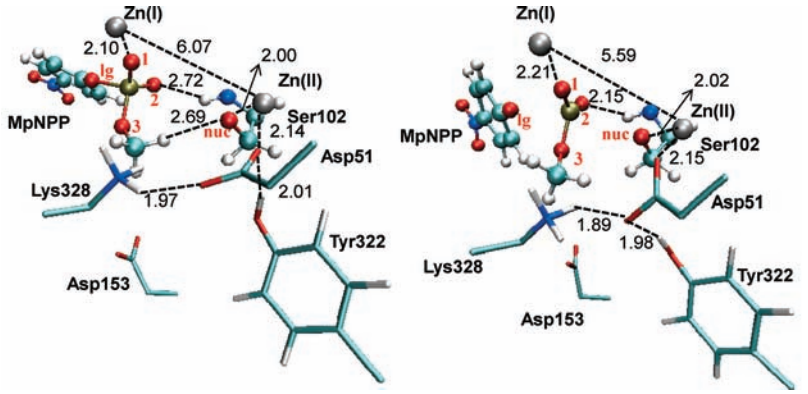

Figure 7. Representative snapshots of the reactant state (left) and TS (right) for the reaction of hydrolysis of MpNPP in the active site of E322Y AP. Averaged distances are given in Å.

severely reduced from 1.8 × 10^7 M^{-1}·s^{-1} in WT AP to 35 M^{-1}·s^{-1} in the E322Y AP mutant. This dramatic reduction means that the free energy barrier measured from free enzyme and substrate in solution ($\Delta G^{\ddagger}_{E}$) is increased by 7.9 kcal·mol^{-1}.

We obtained the corresponding PMF for the hydrolysis reaction of MpNPP in the active site of the E322Y AP mutant following the same protocol than for WT AP. The free energy barriers from the Michaelis complex, $\Delta G^{\ddagger}_{cat}$ determined for E322Y and WT AP and other mutants that will be analyzed below, are provided in Table 3. The free energy profiles are given as Supporting Information (Figure S2).

These free energy barriers cannot be directly compared to the experimental values because they differ in the binding free energy. However, if the mutation does not drastically alter the binding free energy, then there should be a parallelism in the change of the free energy barriers measured from Michaelis complex or from free enzyme and substrate. This seems to be the case for this enzyme: the value calculated for $\Delta G^{\ddagger}_{cat}$ in E322Y mutant (Table 3) is 1.4 kcal·mol^{-1} lower than the value obtained for WT AP (Table 1). This trend agrees with the observed reduction in the values of $\Delta G^{\ddagger}_{E}$ by 0.4 kcal·mol^{-1} as determined from the experimental second-order rate constants.

Figure 7 shows snapshots of the reactant and transition states of MpNPP in the active site of E322Y AP with averaged values of some key distances. Important changes take place in the active site of AP when this enzyme does not bind the Mg^{2+} ion. The water molecules of the coordination shell of the ion are not found in the active site of the mutant, and Asp51 is no longer bridging between the Mg^{2+} and the Zn(II) centers. As observed in Figure 7, Asp51 now establishes a hydrogen-bond interaction with Lys328 and displaces this residue from the neighborhood of the methyl group. It is important to point out that this interaction observed in our simulations between Lys328 and Asp51 is not found in the X-ray structure of the E322Y AP mutant.[22] This enzyme is crystallized with an inorganic phosphate anion in the active site that establishes a water-mediated interaction with Lys328. This interaction is not observed when the diester is placed in the active site. Instead, Lys328 establishes a strong interaction with Asp51 in the E322Y mutant. The displacement of Lys328, together with the absence of the water molecules coordinated to the Mg^{2+} ion, makes room in the active site to place the methyl group of MpNPP, especially at the TS when the phosphate group must be inverted. The consequence is a moderate reduction of the activation free energy as reflected in the experimental rate constants and the calculated activation free energies.

According to our interpretation of the results obtained for the E322Y AP mutant, the deletion of the Mg^{2+} ion of the active site has direct and indirect consequences on the ability of the active site to catalyze the hydrolysis reaction. The direct effect is related to the absence of the coordination water molecules in the active site of the mutant. One of these water molecules plays an important role stabilizing one of the nonbridging oxygen atoms of the monoester in the wild type enzyme (see Figure 1A). This would explain the considerable reduction of the monoestarase activity in the mutant.[22] The calculated free energy profile associated to the breaking of the P−O_{lg} bond of mNBP in the active site of the mutant shows a free energy barrier $\Delta G^{\ddagger}_{cat}$ of 20.4 kcal·mol^{-1}; this is 10.0 kcal·mol^{-1} higher than in WT AP (see Supporting Information, Figure S3), in reasonable agreement

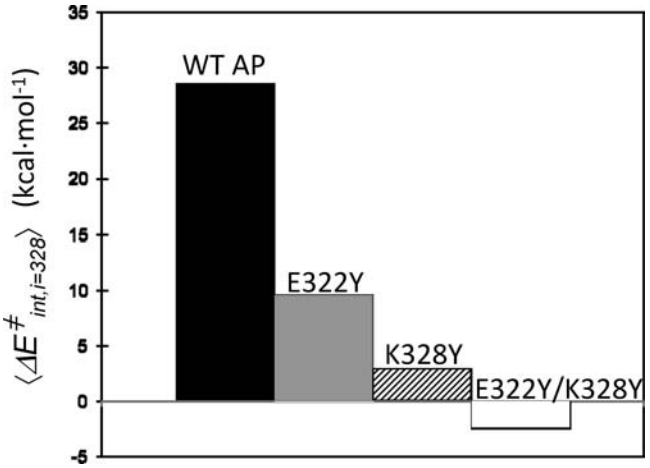

Figure 8. Averaged contribution of the interaction energy of residue 328 with the reacting system (Ser102 + MpNPP) to the energy barrier of hydrolysis of MpNPP catalyzed by WT AP and several mutants.

with the increase of 7.9 kcal·mol^{-1} observed from the second-order rate constants. The indirect effect is due to the displacement of Lys328 when a diester is placed in the active site of the mutant. In such a case Lys328 can be alternatively stabilized by Asp51, a residue that is not available in WT AP because that residue is found bridging between Zn(II) and the Mg^{2+} centers (see Figure 1A). As a result, there is more room in the active site to place the alkyl group of the diester and then Lys328 makes a smaller contribution to the energy barrier of diester hydrolysis in E322Y mutant than in WT AP. This is reflected in the differences between the averaged values of the interaction energy of residue 328 with the reacting system at the transition and reactant states obtained for WT AP, E322Y AP, and other mutants represented in Figure 8.

Another interesting change found in the E322Y mutant is the coordination of the covalent intermediate obtained in this reaction step. In the mutant, after crossing the TS region, the reaction proceeds with the nucleophile leaving the coordination shell of Zn(II) and approaching the methylphosphate group that remains bound to Zn(I). Then the enzyme−methylphosphate intermediate is found in the coordination shell of Zn(I) as shown in Scheme 2 (E·P intermediate II). The deletion of the positive charge associated to the Mg^{2+} ion, absent in the E322Y mutant, obviously favors the displacement of the nucleophile toward the phosphate group, while this remains coordinated to Zn(I). This coordination of the covalent intermediate is different to that found in WT AP (intermediate I).

Conclusions obtained from the study of E322Y mutation encouraged us to analyze the consequences of an in silico mutation of Lys328. This residue stabilizes both the reactants and TS of mNBP hydrolysis in AP to a similar extent, and the contribution of its interaction energy to the barrier, computed according to eq 3, is small, −1.1 kcal·mol^{-1}, while the effect on the barrier for MpNPP hydrolysis is 26.8 kcal·mol^{-1}, as observed in Figure 8. Mammalian and yeast APs have a histidine instead of lysine in the equivalent position.[60] *E. coli* AP mutants where Lys328 was substituted by histidine (K328H)[60−62] or tryptophan (K328W)[62,63] present monoesterase activity. In agreement with our findings, the study of the K328H AP mutant showed that the Lys328 most probably play an important role in substrate and product binding, but its mutation does not reduce the catalytic properties of *E. coli* AP.[64] We then decided to study the effect of the mutation of Lys328 on the diesterase activity of *E. coli*. The residue occupying the equivalent position in diesterase NPP is Glu211. This residue is negatively charged, and instead of remaining close to the substrate it is oriented outward the active site. The substitution of Lys328 by a negatively charged residue could provoke large perturbations in the protein structure, which are difficult to sample adequately in our simulations. For this reason we decided to substitute Lys328 by an uncharged residue, a tyrosine. Tyrosine, a residue of similar size to histidine, is able to establish hydrogen-bond interactions in the active site and contains an aromatic ring that can make favorable contact with the methyl group.[65,66] The free energy barrier obtained for the K328Y AP mutant (12.0 kcal·mol^{-1}) is smaller to that of WT AP (13.5 kcal·mol^{-1}) and very similar to that obtained for E322Y (12.1 kcal·mol^{-1}). The free energy barrier and averaged values of the bond to be broken and the bond to be formed are provided in Table 3. The TS structure is presented in Figure 9, and the contribution of the interaction energy of residue Tyr328 with the reacting system to the energy barrier is depicted in Figure 8. When Lys328 is mutated to tyrosine, this residue makes a smaller unfavorable contribution to the energy barrier, resulting in an increased activity of K328Y AP with diesters with respect to the WT AP (see Table 3). Tyr328 maintains a water-mediated interaction with Asp153, which in turn is hydrogen-bonded to one of the water molecules of the coordination shell of the Mg^{2+} center. This network of water-mediated interactions gives more room to the placement of the methyl group, especially at the TS, when the phosphate group must be inverted, as reflected in the larger distance between the water molecule coordinated to the Mg^{2+} ion and the esterified oxygen atom (O3).

One important difference found between the reaction mechanisms determined in K328Y AP and in wt or E322Y APs is the coordination of the covalent enzyme−methylphosphate intermediate complex. As explained above, this intermediate remains bound to Zn(I) and Zn(II) in the case of WT AP (E·P intermediate I in Scheme 2) and only to Zn(I) in the case of E322Y mutant (E·P intermediate II in Scheme 2). In the K328Y AP mutant, the methylphosphate group leaves the coordination shell of Zn(I) and approaches Ser102 to form the new P−O_{nuc} bond. The covalent intermediate formed is then coordinated to Zn(II) instead of Zn(I) as shown in Scheme 2 (intermediate III). The obtained covalent intermediate is then more buried into the active site, and this could affect the rate of the subsequent hydrolysis step, which leads to the regenerated enzyme and the corresponding phosphomonoester. According to these findings Lys328 could play an important role anchoring the phosphate group in the coordination shell of Zn(I).

As shown above, specificity for monoesterase or diesterase activity could be the consequence of the interactions established through the O3 oxygen atom of the phosphate group. When a monoester is placed in the active site of WT AP, this oxygen atom can establish interactions with a water molecule present in the coordination shell of the Mg^{2+} and with Lys328. Obviously, the next step in our analysis of the diesterase activity of AP is to carry out a double mutation in which these two interactions disappear. The double AP mutant E322Y/K328Y is the natural choice. We obtained the PMF corresponding to the hydrolysis of MpNPP in the active site of this mutant. The free energy barrier is smaller than in any of the single mutants (see Table 3). The TS for the reaction of the phosphodiester hydrolysis in this double mutant is shown in Figure 9 together with some key averaged distances. In this case, Tyr328 establishes a water-mediated interaction with

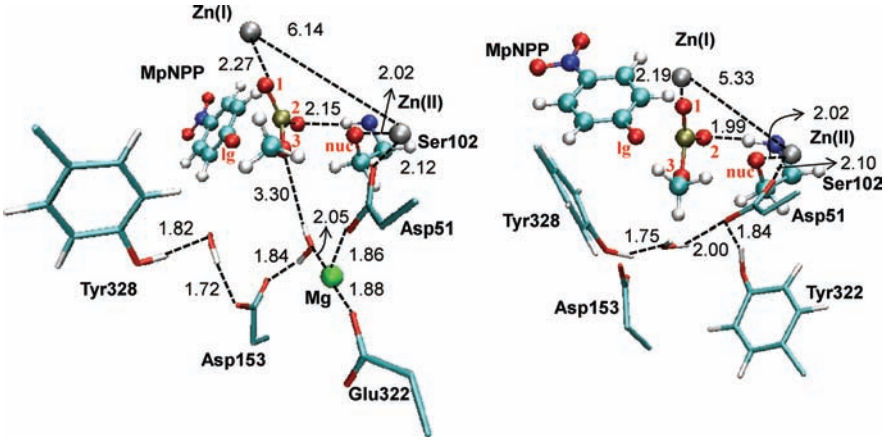

Figure 9. Representative snapshots of the TS's for the reaction of hydrolysis of MpNPP in the active site of K328Y AP (left) and K328Y/E322Y AP (right). Averaged distances are given in Å.

Asp51. In the double mutant, this interaction provokes a rotation of the side chain of Tyr328 at the TS, confronting the aromatic ring to the methyl group in such a way that now, the contribution of the interaction energy of this residue with the reacting system reduces the energy barrier (as seen in Figure 8). After reaching the TS this reaction step is completed when the methylphosphate group leaves the coordination shell of Zn(I) and approaches Ser102 which remains bound to Zn(II) (E·P intermediate III in Scheme 2). This result would confirm the proposed role of Lys328 contributing to anchor the phosphate group in the coordination shell of Zn(I).

4. CONCLUSIONS

We have analyzed the hydrolysis reaction of a phosphodiester (MpNPP) in the active site of a phosphomonoesterase (AP) and several mutants to understand the origin of the promiscuity shown by the enzymes that belong to the AP superfamily. Hybrid QM/MM MD simulations provide atomistic details of the reactions that can be used to rationalize the origin of this promiscuity and then to trace the path followed by evolution to specialize different enzymes in the catalysis of different reactions or different substrates.

The first general conclusion, by comparison with our previous studies, is that alkaline hydrolysis of MpNPP takes place following different mechanisms in aqueous solution and in the active sites of two different members of the AP superfamily. Thus, the reaction mechanism is associative in aqueous solution and dissociative in two enzymes, a monoesterase (AP) and a diesterase (NPP). The free energy barrier obtained for the reaction in AP lies in between the value obtained in aqueous solution and in NPP, in agreement with the experimental observation that AP is able to catalyze the reaction but not as efficiently as the natural phosphodiesterase, NPP. According to our mechanistic findings, the ability shown by AP to catalyze the hydrolysis of both mono and diesters is not really a promiscuity of reaction, since the nature of the reaction mechanisms remains unaltered in both cases. Our QM/MM studies support a picture of the evolution of the AP superfamily in which the reaction mechanism is maintained for different substrates.

An important feature observed when placing MpNPP in AP active site is the interaction established between the methyl group of the phosphodiester and the nucleophilic oxygen atom, which contribute to stabilize the reactants with respect to the TS. The analysis based in our QM/MM models also supports the hypothesis of Herschlag and co-workers.[22] The interactions established by one of the oxygen atoms of the phosphate group with the coordination shell of the Mg^{2+} ion and with Lys328 could be decisive to differentiate between monoesters and diesters. Strong hydrogen-bond interactions are found only when the oxygen atom of the phosphate group placed in the surroundings of these residues does not bear an alkyl group, this is for monoesters. This explanation was tested with different AP mutants: E322Y, which does not bound Mg^{2+} ions, K328Y, where Lys328 is mutated to an uncharged residue and the double mutant E322Y/K328Y, where both effects are combined. Only the first mutant has been experimentally studied, finding that the monoesterase activity is dramatically diminished when compared to the WT AP while the diesterase activity is slightly augmented. Our results explain these changes associated to the mutation because deletion of the Mg^{2+} ion does not only eliminate the water molecules of its coordination shell, diminishing the monoesterase activity, but also provokes a displacement of Lys328, increasing then the diesterase activity. Conversely, mutation of Glu211 and/or Tyr205 in NPP could increase the monoesterase activity of this enzyme.

In addition, the results of our simulations can be also used to explain the ability of this enzyme to catalyze the hydrolysis of different substrates having very different leaving groups (substrate promiscuity). We show, here and in previous studies with other leaving groups, that the charge on the leaving group at the TS can be stabilized in different forms: by means of the Zn(I) ion or by means of other residues placed at the outer side of the active site (such as Lys167) depending on the nature of the leaving group.

All in all, these findings reveal the molecular basis of the evolution in the AP superfamily. These enzymes, evolved from a common ancestor, display preferential activity for diesters or monoesters by means of specific interactions that do not involve the zinc sites, but conserved promiscuous activity because the reaction mechanism, based on the characteristics of the bimetallo active site, is maintained.

■ ASSOCIATED CONTENT

Supporting Information. Figures presenting the location of Arg166 and Lys167 in the reactants and transition states of the

MpNPP hydrolysis in AP, coordinates of a representative structure of the reactant state and TS in PDB format, and PMFs obtained for the hydrolysis of MpNPP in WT AP and the mutants analyzed in this paper and for the hydrolysis of mNBP in WT AP and E322Y AP. This material is available free of charge via the Internet at http://pubs.acs.org.

AUTHOR INFORMATION

Corresponding Author
ignacio.tunon@uv.es;moliner@uji.es

5. ACKNOWLEDGMENT

This work was supported by the Ministerio de Ciencia e Innovación, project CTQ2009-14541-C02, by Generalitat Valenciana, Prometeo/2009/053 and ACOMP/2011/028, and by Universitat Jaume I-Bancaixa foundation, project P1-1B2008-38. V.L.-C. and M.R. thank the Ministerio Ciencia e Innovación for a doctoral grant and a "Juan de la Cierva" contract, respectively. The authors acknowledge computational facilities of the Servei d'Informàtica de la Universitat de València in the "Tirant" supercomputer, which is part of the Spanish Supercomputing Network.

REFERENCES

(1) Gerlt, J. A.; Babbitt, P. C. *Annu. Rev. Biochem.* **2001**, *70*, 209–246.
(2) O'Brien, P. J.; Herschlag, D. *Chem. Biol.* **1999**, *6*, R91–R105.
(3) Khersonsky, O.; Roodveldt, C.; Tawfik, D. S. *Curr. Opin. Chem. Biol.* **2006**, *10*, 498–508.
(4) Jensen, R. A. *Annu. Rev. Microbiol.* **1976**, *30*, 409–425.
(5) Zalatan, J. G.; Herschlag, D. *J. Am. Chem. Soc.* **2006**, *128*, 1293–1303.
(6) Boyer, P. D.; Cross, R. L.; Momsen, W. *Proc. Natl. Acad. Sci. U.S. A.* **1973**, *70*, 2837–2839.
(7) Admiraal, S. J.; Herschlag, D. *Chem. Biol.* **1995**, *2*, 729–739.
(8) Cleland, W. W.; Hengge, A. C. *Chem. Rev.* **2006**, *106*, 3252–3278.
(9) Benkovic, S. J.; Schray, K. J. In *The Enzymes*; Boyer, P. D., Ed.; Academic Press: New York, 1973; Vol. III; pp 201−238.
(10) Vetter, I. R.; Wittinghofer, A. *Q. Rev. Biophys.* **1999**, *32*, 1–56.
(11) Ahn, N. *Chem. Rev.* **2001**, *101*, 2207–2208.
(12) Zalatan, J. G.; Catrina, I.; Mitchell, R.; Grzyska, P. K.; O'Brien, P. J.; Herschlag, D.; Hengge, A. C. *J. Am. Chem. Soc.* **2007**, *129*, 9789–9798.
(13) Catrina, I.; O'Brien, P. J.; Purcell, J.; Nikolic-Hughes, I.; Zalatan, J. G.; Hengge, A. C.; Herschlag, D. *J. Am. Chem. Soc.* **2007**, *129*, 5760–5765.
(14) Nikolic-Hughes, I.; Rees, D. C.; Herschlag, D. *J. Am. Chem. Soc.* **2004**, *126*, 11814–11819.
(15) Yang, K. C.; Metcalf, W. W. *Proc. Natl. Acad. Sci. U.S.A.* **2004**, *101*, 7919–7924.
(16) O'Brien, P. J.; Herschlag, D. *Biochemistry* **2001**, *40*, 5691–5699.
(17) Coleman, J. E. *Annu. Rev. Biophys. Biomol. Struct.* **1992**, *21*, 441–483.
(18) Stefan, C.; Jansen, S.; Bollen, M. *Trends Biochem. Sci.* **2005**, *30*, 542–550.
(19) Goding, J. W.; Grobben, B.; Slegers, H. *Biochim. Biophys. Acta* **2003**, *1638*, 1–19.
(20) Zalatan, J. G.; Fenn, T. D.; Brunger, A. T.; Herschlag, D. *Biochemistry* **2006**, *45*, 9788–9803.
(21) Lassila, J. K.; Herschlag, D. *Biochemistry* **2008**, *47*, 12853–12859.
(22) Zalatan, J. G.; Fenn, T. D.; Herschlag, D. *J. Mol. Biol.* **2008**, *384*, 1174–1189.
(23) Kim, E. E.; Wyckoff, H. W. *J. Mol. Biol.* **1991**, *218*, 449–464.
(24) Stec, B.; Holtz, K. M.; Kantrowitz, E. R. *J. Mol. Biol.* **2000**, *299*, 1303–1311.
(25) Klahn, M.; Rosta, E.; Warshel, A. *J. Am. Chem. Soc.* **2006**, *128*, 15310–15323.
(26) Rosta, E.; Kamerlin, S. C. L.; Warshel, A. *Biochemistry* **2008**, *47*, 3725–3735.
(27) Zalatan, J. G.; Catrina, I.; Mitchell, R.; Grzyska, P. K.; O'Brien, P. J.; Herschlag, D.; Hengge, A. C. *J. Am. Chem. Soc.* **2007**, *129*, 9789–9798.
(28) Hollfelder, F.; Herschlag, D. *Biochemistry* **1995**, *34*, 12255–12264.
(29) McWhirter, C.; Lund, E. A.; Tanifum, E. A.; Feng, G.; Sheikh, Q. I.; Hengge, A. C.; Williams, N. H. *J. Am. Chem. Soc.* **2008**, *130*, 13673–13682.
(30) Martí, S.; Moliner, V.; Tuñón, I. *J. Chem. Theory Comput.* **2005**, *1*, 1008–1016.
(31) Gao, J. In *Reviews in Computational Chemistry*; Kenny, B., Lipkowitz, D. B. B., Eds.; Wiley: New York, 1995; pp 119−185.
(32) Warshel, A.; Levitt, M. *J. Mol. Biol.* **1976**, *103*, 227–249.
(33) Gao, J. L.; Truhlar, D. G. *Annu. Rev. Phys. Chem.* **2002**, *53*, 467–505.
(34) López-Canut, V.; Martí, S.; Bertrán, J.; Moliner, V.; Tuñón, I. *J. Phys. Chem. B* **2009**, *113*, 7816–7824.
(35) López-Canut, V.; Ruiz-Pernía, J.; Tuñón, I.; Ferrer, S.; Moliner, V. *J. Chem. Theory Comput.* **2009**, *5*, 439–442.
(36) López-Canut, V.; Roca, M.; Bertrán, J.; Moliner, V.; Tuñón, I. *J. Am. Chem. Soc.* **2010**, *132*, 6955–6963.
(37) Antosiewicz, J.; McCammon, J. A.; Gilson, M. K. *J. Mol. Biol.* **1994**, *238*, 415–436.
(38) Field, M. J.; Amara, P.; David, L.; Rinaldo, D., Laboratoire de Dynamique Moleculaire, Institut de Biologie Structurale, Grenoble, France, Personal communication, 2004.
(39) O'Brien, P. J.; Herschlag, D. *Biochemistry* **2002**, *41*, 3207–3225.
(40) Bas, D. C.; Rogers, D. M.; Jensen, J. H. *Proteins: Struct., Funct., Bioinf.* **2008**, *73*, 765–783.
(41) Li, H.; Robertson, A. D.; Jensen, J. H. *Proteins: Struct., Funct., Bioinf.* **2005**, *61*, 704–721.
(42) Singh, U. C.; Kollman, P. A. *J. Comput. Chem.* **1986**, *7*, 718–730.
(43) Field, M. J.; Bash, P. A.; Karplus, M. *J. Comput. Chem.* **1990**, *11*, 700–733.
(44) Nam, K.; Cui, Q.; Gao, J. L.; York, D. M. *J. Chem. Theory Comput.* **2007**, *3*, 486–504.
(45) Nam, K.; Gao, J. L.; York, D. M. *J. Am. Chem. Soc.* **2008**, *130*, 4680–4691.
(46) Pranata, J.; Wierschke, S. G.; Jorgensen, W. L. *J. Am. Chem. Soc.* **1991**, *113*, 2810–2819.
(47) Jorgensen, W. L.; Tirado-Rives, J. *J. Am. Chem. Soc.* **1988**, *110*, 1657–1666.
(48) Jorgensen, W. L.; Chandrasekhar, J.; Madura, J. D.; Impey, R. W.; Klein, M. L. *J. Chem. Phys.* **1983**, *79*, 926–935.
(49) Field, M. J. *A Practical Introduction to the Simulation of Molecular Systems*, 1st ed.; Cambridge University Press: Cambridge, U.K., 1999.
(50) Roux, B. *Comput. Phys. Commun.* **1995**, *91*, 275–282.
(51) Torrie, G. M.; Valleau, J. P. *J. Comput. Phys.* **1977**, *23*, 187–199.
(52) Kumar, S.; Bouzida, D.; Swendsen, R. H.; Kollman, P. A.; Rosenberg, J. M. *J. Comput. Chem.* **1992**, *13*, 1011–1021.
(53) Pauling, L. *The Nature of the Chemical Bond*; Cornell University Press: Ithaca, NY, 1960.
(54) Representative snapshots are selected on the basis of the mean square deviations of some distances to the average values. Selected distances include the bond breaking and forming distances and hydrogen bond distances analyzed in the text.
(55) Gu, Y. L.; Kar, T.; Scheiner, S. *J. Am. Chem. Soc.* **1999**, *121*, 9411–9422.
(56) Pedzisa, L.; Hay, B. P. *J. Org. Chem.* **2009**, *74*, 2554–2560.
(57) Zhao, Y.; Truhlar, D. G. *Theor. Chem. Acc.* **2008**, *120*, 215–241.
(58) Frisch, M. J.; Headgordon, M.; Pople, J. A. *Chem. Phys. Lett.* **1990**, *166*, 275–280.

(59) Frisch, M. J.; Headgordon, M.; Pople, J. A. *Chem. Phys. Lett.* **1990**, *166*, 281–289.
(60) Murphy, J. E.; Tibbitts, T. T.; Kantrowitz, E. R. *J. Mol. Biol.* **1995**, *253*, 604–617.
(61) Kaneko, Y.; Hayashi, N.; Tohe, A.; Banno, I.; Oshima, Y. *Gene* **1987**, *58*, 137–148.
(62) Xu, X.; Kantrowitz, E. R. *Biochemistry* **1991**, *30*, 7789–7796.
(63) Hulett, F. M.; Kim, E. E.; Bookstein, C.; Kapp, N. V.; Edwards, C. W.; Wyckoff, H. W. *J. Biol. Chem.* **1991**, *266*, 1077–1084.
(64) Murphy, J. E.; Kantrowitz, E. R. *Mol. Microbiol.* **1994**, *12*, 351–357.
(65) Shibasaki, K.; Fujii, A.; Mikami, N.; Tsuzuki, S. *J. Phys. Chem. A* **2006**, *110*, 4397–4404.
(66) Note that a bulkier R′ group could require a different selection to replace Lys328.